



# Correlation of Microwave Dielectric Properties and Normal Vibration Modes of $\text{Ba}(\text{Mg}_{1/3}\text{Ta}_{2/3})\text{O}_3$ -Series Materials

YI-CHUN CHEN,<sup>1,3</sup> HSIU-FUNG CHENG,<sup>\*,1</sup> CHIA-CHI LEE,<sup>1</sup> CHIH-TA CHIA,<sup>1</sup>  
HSIANG-LIN LIU<sup>1</sup> & I-NAN LIN<sup>2</sup>

<sup>1</sup>Department of Physics, National Taiwan Normal University, Taipei 116, Taiwan, Republic of China

<sup>2</sup>Department of Physics, Tamkang University, Tamsui 251, Taiwan, Republic of China

<sup>3</sup>Institute of Physics, Academia Sinica, Taipei 115, Taiwan, Republic of China

Submitted March 26, 2003; Revised February 7, 2004; Accepted February 9, 2004

**Abstract.** Microwave dielectric properties of  $\text{Ba}(\text{Mg}_{1/3}\text{Ta}_{2/3})\text{O}_3$ -series materials were investigated using Fourier transform infrared spectroscopy (FTIR) and Raman spectroscopy. The normal vibration modes of these spectra were assigned, and the origin of dielectric response of the materials was deduced. Among the prominent normal vibration modes in the FTIR spectra, those which correlated with O-layers and Ba-layers change with Sr-ratio most significantly, whereas in micro-Raman measurements, the  $A_{1g}(\text{O})$  phonon of oxygen-octahedron stretch mode changes with Sr-ratio most profoundly. These results reveal clearly the close relationship between the characteristics of FTIR and Raman spectra of the BMT-series materials and their microwave dielectric properties.

**Keywords:** microwave dielectrics, Raman spectroscopy, FTIR spectroscopy

## 1. Introduction

Complex perovskite compounds with chemical formula  $\text{Ba}(\text{B}'_{1/3}\text{B}''_{2/3})\text{O}_3$ , where  $\text{B}' = \text{Zn, Mg, Ni or Mn}$  and  $\text{B}'' = \text{Nb or Ta}$ , exhibit ultra-low dielectric losses at microwave frequencies [1–3], when the materials possess  $\text{B}'\text{-B}''$  1:2 ordered arrangement with the symmetry of the structure described by the  $P\bar{3}m1 (D_{3d}^3)$  space group [4]. Since the dielectric properties at microwave frequencies are mainly contributed from the ionic polarization, the study of phonon vibration spectra of  $\text{Ba}(\text{B}'_{1/3}\text{B}''_{2/3})\text{O}_3$  has been of particular interest [5–12]. Recently, the Raman phonons [13] and the normal mode for resonant peaks in FTIR spectra [14] in  $\text{Ba}(\text{Mg}_{1/3}\text{Ta}_{2/3})\text{O}_3$ - $\text{Ba}(\text{Mg}_{1/3}\text{Nb}_{2/3})\text{O}_3$ , BMT-BMN, materials were unambiguously identified. The change in microwave dielectric properties of the BMT-BMN materials with the composition has been correlated with the modification on Raman and FTIR spectroscopic characteristics. However, the genuine

mechanism on modifying these spectroscopic behaviors is still not clear.

In this study, we investigated the evolution of the crystal structure of  $(1-x)\text{Ba}(\text{Mg}_{1/3}\text{Ta}_{2/3})\text{O}_3$ - $x\text{Sr}(\text{Mg}_{1/3}\text{Ta}_{2/3})\text{O}_3$ ,  $(1-x)\text{BMT}$ - $x\text{SMT}$  materials with the composition using Rietvelt method [15], so as to understand the factor which alters the Raman and FTIR spectroscopic characteristics for these materials. By analyzing phonon properties, we attempted to explain the modification on the normal vibration modes for  $(1-x)\text{BMT}$ - $x\text{SMT}$  due to the change on composition and to correlate the dispersion parameters of the normal modes with their microwave dielectric properties.

## 2. Experimental Details

The  $(1-x)\text{BMT}$ - $x\text{SMT}$  ceramic samples with  $x = 0, 1/8, 2/8, 3/8, \text{ and } 4/8$  were prepared by conventional mixed oxide process. These samples were conventionally sintered at  $1600^\circ\text{C}$  for 3 h. Far-infrared and mid-infrared reflectance spectra, from 20 to  $800\text{ cm}^{-1}$  were taken at room temperature using a Bruker IFS 66v

\*To whom all correspondence should be addressed. E-mail: hfcheng@phy03.phy.ntnu.edu.tw

Fourier transform infrared spectrometer. The dielectric properties were calculated from Kramers-Kronig analysis of the reflectance data [13]. Raman measurements were performed at room temperature, and signals were recorded by a DILOR XY-800 triple grating Raman spectrometer with the resolution around  $0.5 \text{ cm}^{-1}$ . The dielectric properties were measured by  $\text{TE}_{011}$  resonant cavity method using HP 8722 network analyzer, in the vicinity of 6 GHz.

### 3. Results and Discussions

The  $\text{Ba}(\text{Mg}_{1/3}\text{Ta}_{2/3})\text{O}_3$ , BMT perovskite structure was markedly distorted due to the ordering of Mg and Ta cations, such that the symmetry of the unit cells change from  $Pm\bar{3}m$  to  $P\bar{3}m1$ . Three consecutive cubes are required to completely describe a unit cell of the BMT materials (Fig. 1(a)), which are better described

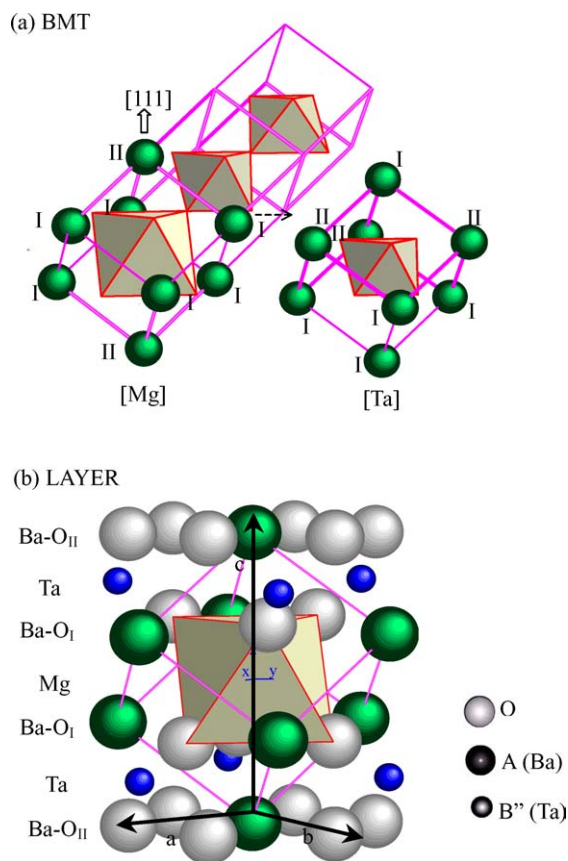


Fig. 1. Schematics showing the crystal structure of a  $\text{Ba}(\text{Mg}_{1/3}\text{Ta}_{2/3})\text{O}_3$  material: (a) an unit cell containing 3 consecutive perovskite cubes and (b) hexagonal lattice of the same unit cell.

by a hexagonal lattice illustrated in Fig. 1(b). Detailed analysis using Rietvelt method [15] reveals a very interesting results, viz. the size of Mg—O octahedrons is markedly larger than that of Ta—O octahedrons ( $d_{\text{Mg}} = 2.51 \text{ \AA}$ ,  $d_{\text{Ta}} = 2.29 \text{ \AA}$ ). Large difference in Ta—O and Mg—O octahedron size is probably the factor resulting in intrinsically high degree of ordering for BMT materials. Incorporating Sr-ions to replace for the Ba-ions reduces the lattice parameters slightly, without altering the size of Mg- and Ta-octahedrons (not shown).

Raman spectroscopy shown in Fig. 2 reveals that all the samples possess very sharp phonon resonance peak, indicating again that these materials are highly ordered. The Raman active modes have been unambiguously assigned [13] and are listed in Table 1(a), in which the effect of Sr-incorporation on the characteristics of the BMT materials is also summarized. Among the major Raman peaks observed in Fig. 2, the  $A_{1g}[\text{O}]$  breathing modes at  $797 \text{ cm}^{-1}$  shows largest width and most pronounced blue-shifting with Sr-ratio (i.e., toward higher frequency), where the Sr-ratio is defined as  $r = [\text{Sr}]/([\text{Sr}] + [\text{Ba}])$ . The relatively large width of  $A_{1g}[\text{O}]$  breathing mode can apparently be ascribed to the co-existence of the two octahedrons (Mg-oct. and Ta oct.), which vibrate incoherently in response to the external excitation. The increase in width of this mode with Sr-ratio infers that the coherency of the two

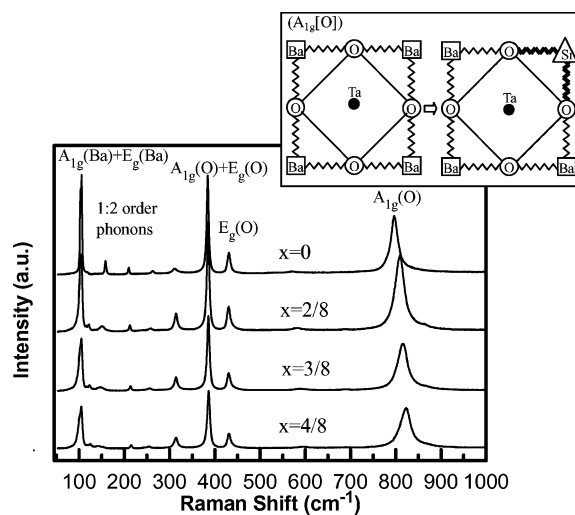


Fig. 2. Raman spectra of  $(1-x)\text{Ba}(\text{Mg}_{1/3}\text{Ta}_{2/3})\text{O}_3-x\text{Sr}(\text{Mg}_{1/3}\text{Ta}_{2/3})\text{O}_3$  materials with  $x=0, 2/8, 3/8$  and  $4/8$  (the inset shows the effective force constant experienced by oxygen ions of an oxygen cage).

Table 1. The effect of Sr-incorporation on the characteristic of (a) Raman spectroscopy and (b) FTIR spectroscopy.

	Frequency (cm <sup>-1</sup> )	Assignment	Remark
(a) Raman peak <sup>a</sup>			
$\omega_{01}$	104	E <sub>g</sub> [Ba/Sr]	Broadening
$\omega_{02}$	106	A <sub>g</sub> [Ba/Sr]	Broadening
$\omega_{03}$	158	E <sub>g</sub> [O]	Invariant
$\omega_{04}$	211	E <sub>g</sub> [Ta]	Invariant
$\omega_{05}$	264	A <sub>1g</sub> [Ta]	Invariant
$\omega_{06}$	385	A <sub>1g</sub> [O] + E <sub>g</sub> [O]	Invariant
$\omega_{07}$	432	E <sub>g</sub> [O]	Invariant
$\omega_{08}$	797	A <sub>1g</sub> [O]	Blue-shifting
(b) FTIR peak <sup>a</sup>			
$\omega_{02}$	137.3	A <sub>2u</sub> [Ta]	Invariant
$\omega_{04}$	218.1	E <sub>u</sub> [O <sub>II</sub> ]	Invariant
$\omega_{05}$	242.2	A <sub>2u</sub> [O <sub>II</sub> ]	Invariant
$\omega_{06}$	217.3	E <sub>u</sub> [Mg]	Invariant
$\omega_{07}$	313.2	A <sub>2u</sub> [Ba/Sr]	Blue-shifting
$\omega_{012}$	518.2	E <sub>u</sub> [O <sub>I</sub> ]	Blue-shifting
$\omega_{014}$	605.2	A <sub>2u</sub> [O <sub>I</sub> ]	Blue-shifting

<sup>a</sup>The assignment of Raman resonance peaks follows Ref. 15 and the assignment of FTIR resonance peaks follows Ref. 16.

octahedrons deteriorate as Sr-ions were incorporated into BMT materials, which is probably due to the decrease on the ordering of the two octahedrons.

The blue shifting of A<sub>1g</sub>[O] mode with Sr-ratio indicates that the breathing of Ta—O (or Mg—O) octahedrons is not only affected by the Ta—O (or Mg—O) bond strength inside the octahedron cage, but also influenced by the bond strength between O-ions and Ba(Sr)-ions, which are sitting external to the octahedron, at the corners of the perovskite cube. Blue-shifting infers that incorporation of Sr-ions to partially replace for the Ba-ions and hence increases the strength of Ba(Sr)—O bonds, which increases the effective force constant experienced by the oxygen ions (depicted in inset of Fig. 2). The other important phenomenon resulted from the Sr-ions incorporation is splitting of Raman resonance peak in the vicinity of the A<sub>1g</sub>[Ba]+E<sub>g</sub>[Ba] resonance mode at around 105 cm<sup>-1</sup>, which results in broadening of the effective width of these Raman resonance peaks. Moreover, the strength of the 1:2 order phonons locating at around 150–300 cm<sup>-1</sup>, (E<sub>g</sub>[Ta], A<sub>1g</sub>[Ta] and E<sub>g</sub>[O] modes) decreases appreciably with Sr-ratio, which, again, implies the deterioration of the ordering of Ta—O and Mg—O octahedrons.

While the Raman spectroscopy illustrates clearly how the Sr-addition affects the vibrational characteristics of BMT lattices, this behavior can not directly account for the effect of Sr-incorporation on the di-

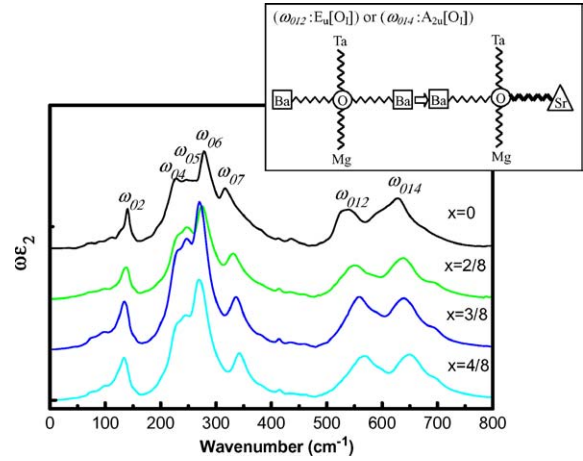


Fig. 3. Fourier transformed infrared (FTIR) spectra of (1 - x)Ba(Mg<sub>1/3</sub>Ta<sub>2/3</sub>)O<sub>3</sub>-xSr(Mg<sub>1/3</sub>Ta<sub>2/3</sub>)O<sub>3</sub> materials with x = 0, 2/8, 3/8 and 4/8 (the inset shows the effective force constant experienced by oxygen ions in Ba—O<sub>I</sub> layer).

electric response of the BMT materials, as the Raman vibration modes are non-polar in these materials. To correlate the lattice vibrational characteristics of the materials with their dielectric behavior, understanding on the polar vibrational modes in Fourier transformed infrared-red spectra (FTIR) is required. Figure 3 shows how the Sr-incorporation affects the FTIR spectroscopy of the BMT materials, which have recently been assigned [14] and the major resonance peaks are listed in Table 1(b).

Among these FTIR resonance peaks, the  $\omega_{07}$ : A<sub>2u</sub>[Ba] at around 313 cm<sup>-1</sup> shows most prominent blue-shift (i.e., toward higher frequency) with Sr-ratio. The  $\omega_{012}$ : E<sub>u</sub>[O<sub>I</sub>] and  $\omega_{015}$ : A<sub>2u</sub>[O<sub>I</sub>] at around 518 and 605 cm<sup>-1</sup>, respectively, also show blue-shift behavior but in a less extend. The blue-shifting of A<sub>2u</sub>[Ba] mode is apparently due to mass loading effect, as the Sr-ions are much lighter than the Ba-ions. The explanation on blue-shifting of E<sub>u</sub>[O<sub>I</sub>]/A<sub>2u</sub>[O<sub>I</sub>] mode is not as straight forward. The major force constant influencing the vibrational characteristics of these modes is Ta—O, Mg—O and Ba(Sr)—O bonds, since the Ba(Sr)—O<sub>I</sub> layer is sandwiched in between Ta- and Mg-layer (inset Fig. 3). The blue-shifting of E<sub>g</sub>[O<sub>I</sub>] and A<sub>2u</sub>[O<sub>I</sub>] modes can thus be ascribed to the increase in Ba(Sr)—O bond, as Ta—O and Mg—O bond strengths are not changing with Sr-ratio.

The same mechanism is expected to influence the vibrational behavior of  $\omega_{04}$ : E<sub>u</sub>[O<sub>II</sub>] and  $\omega_{05}$ : A<sub>2u</sub>[O<sub>II</sub>] modes, but in much less extend, as the Ba-ion to O-ion

ratio is only Ba:O<sub>II</sub> = 1:6 in Ba—O<sub>II</sub> layer, which is much smaller than that in Ba—O<sub>I</sub> layer (Ba:O<sub>I</sub> = 3:3). The E<sub>u</sub>[O<sub>II</sub>] and A<sub>2u</sub>[O<sub>II</sub>] are thus essentially invariant with respect to the Sr-ratio. The other FTIR resonance modes showing invariant behavior are  $\omega_{02}$ : A<sub>2u</sub>[Ta] and  $\omega_{06}$ : E<sub>u</sub>[Mg] modes, which is expected as Sr-incorporation neither alters the mass nor the force constant of the Ta- and Mg related resonators.

To understand the correlation between the lattice vibrational characteristics of the (1 - *x*)BMT-*x*SMT materials with their dielectric properties, the quality factor ( $Q \times f$ ) and the dielectric constant ( $K$ ) of the materials were measured by using a cavity method and are plotted as open and solid symbols in Fig. 4(a), respectively. The quality factor ( $Q \times f$ ) decreases from 100,000 to 60,000, whereas the dielectric constant ( $K$ ) increase monotonously from 24 to 28, as Sr-ratio increases. The dielectric properties at microwave frequencies obtained from K-K analysis extrapolation are shown in Fig.

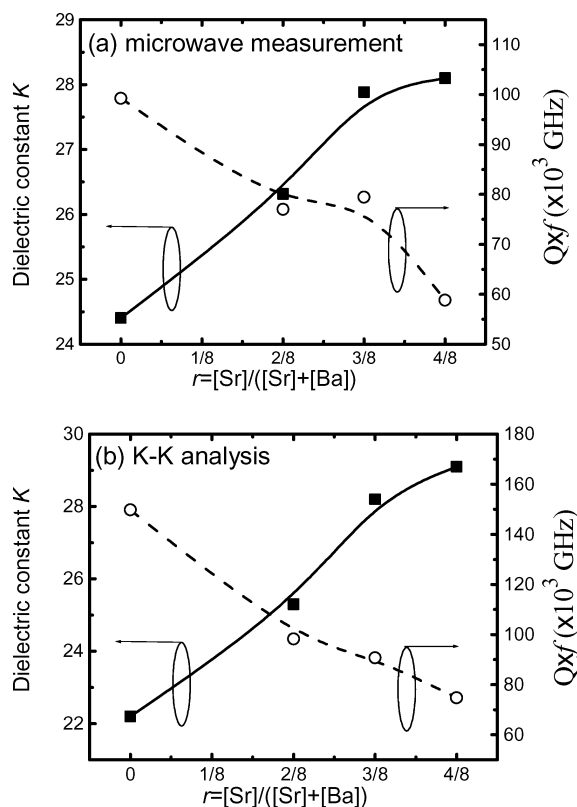


Fig. 4. Variation of quality factor ( $Q$ ) and dielectric constant ( $K$ ) obtained by (a) directly microwave measurement and (b) K-K analysis for (1 - *x*)Ba(Mg<sub>1/3</sub>Ta<sub>2/3</sub>)O<sub>3</sub>-*x*Sr(Mg<sub>1/3</sub>Ta<sub>2/3</sub>)O<sub>3</sub> materials with different Sr-ratio.

4(b) for comparison. Similar trend and order of magnitude implied that microwave dielectric responses are mainly contributed from the ionic polarizations of the lattice vibrations observed in the far infrared frequency region.

The degradation of quality factor ( $Q \times f$ ) of the materials with Sr-content can apparently be ascribed to the deterioration of ordering parameters of the perovskite lattices, which is implied by the pronounced broadening of the resonance peaks induced by Sr-addition for A<sub>1g</sub>[O] mode in Raman spectra and E<sub>u</sub>[O<sub>I</sub>]/A<sub>2u</sub>[O<sub>I</sub>] modes in FTIR spectra. While the decrease in  $Q$ -value of the BMT materials is clearly related to the change in normal mode of the lattices, the correlation between the  $K$ -value of the materials with their vibrational characteristics is not as straightforward.

To correlate the dielectric constant ( $K$ ) of the materials with the lattice vibrational characteristics, dielectric function  $4\pi\rho_j$  of each vibrational peaks should be calculated according to Kramer-Kronig [16] theory. However, understanding the behavior of the major resonant peaks qualitatively still facilitates the comprehension on the mechanism, which increases the dielectric constant ( $K$ ) of the materials due to Sr-substitution. Among the major resonant peaks listed in Table 1(b), all the normal modes showing significant blue-shifting, A<sub>2u</sub>[Ba] and E<sub>u</sub>[O<sub>I</sub>]/A<sub>2u</sub>[O<sub>I</sub>], are the vibration of lattices related to Ba—O<sub>I</sub> layer (cf. Fig 1(b)). The lighter Sr-ions and stronger Sr—O bonds, as compared with Ba-ions and Ba—O bonds, respectively, are the two main factors altering these lattice vibration characteristics. Apparently, the polarizability of these normal modes is also enhanced due to Sr-substitution, which is supported by the phenomenon that the integrated intensity of these resonant peaks increases with Sr-ratio.

#### 4. Conclusions

Effect of Sr-ions incorporation on the lattice vibrational characteristics of (1 - *x*)Ba(Mg<sub>1/3</sub>Ta<sub>2/3</sub>)O<sub>3</sub>-*x*Sr(Mg<sub>1/3</sub>Ta<sub>2/3</sub>)O<sub>3</sub> materials was studied by Raman and FTIR spectroscopies. The fact that Sr-ions are lighter than Ba-ions affects the lattice vibration of Ba(Sr)-layer via mass loading effect and that Sr—O bonding is stronger than Ba—O bonding influences the lattice vibration of Ba—O<sub>I</sub> layer via force constant effect. In Raman spectroscopy, A<sub>1g</sub>[O] mode is the only blue-shifting mode, whereas in FTIR spectroscopy, A<sub>2u</sub>[Ba] and E<sub>u</sub>[O<sub>I</sub>]/A<sub>2u</sub>[O<sub>I</sub>] are the

major modes showing blue-shift. All the other modes change insignificantly with Sr-ratio. While Raman spectroscopy illustrates more clearly how the incorporation of Sr-ions alters the lattice vibration modes of the BMT materials, FTIR spectroscopy correlates much more closely with the increase in dielectric constant ( $K$ ) and degradation in quality ( $Q$ ) of the BMT materials.

### Acknowledgment

Financial support of National Science Council, R. O. C., through the projects no. NSC 91-2622-E-007-027, NSC 91-2112-M-003-024 and NSC 92-2622-E-007-016, NSC 92-2210-E-003-001 is gratefully acknowledged by the authors.

### References

1. S. Nomura, K. Toyama, and K. Kaneta, *Jpn. J. Appl. Phys. Part 2*, **21**, L642 (1982).
2. R. Guo, A.S. Shalla, and L.E. Cross, *J. Appl. Phys.*, **75**, 470 (1994).
3. S. Nomura, T. Konoike, Y. Sakabe, and K. Wakino, *J. Am. Ceram. Soc.*, **67**, 59 (1984).
4. F.S. Galasso, *Structure, Properties and Preparation of Perovskite-Type Compounds* (Pergamon, Oxford, 1969), pp. 13–15, 55.
5. H. Tamura, D.A. Sagala, and K. Wakino, *Jpn. J. Appl. Phys. Part 1*, **25**, 787 (1986).
6. I.G. Siny, R.W. Tao, R.S. Katiyar, R.A. Guo, and A.S. Bhalla, *J. Phys. Chem. Solids*, **59**, 181 (1998).
7. H. Tamura, D. A. Sagala, and K. Wakino, *J. Am. Ceram. Soc.*, **76**, 2433 (1993).
8. K. Tochi and N. Takeuchi, *J. Mater. Sci. Lett.*, **8**, 1144 (1989).
9. T. Nagai, M. Sugiyama, M. Sando, and K. Nihara, *Jpn. J. Appl. Phys. Part 1*, **35**, 5163 (1996).
10. K. Tochi and N. Takeuchi, *J. Mater. Sci. Lett.*, **7**, 1080 (1988).
11. K. Tochi, N. Takeuchi, and S. Emura, *J. Am. Ceram. Soc.*, **72**, 158 (1989).
12. N. Sugiyama and T. Nagai, *Jpn. J. Appl. Phys. Part 1*, **32**, 4360 (1993).
13. C.T. Chia, Y.C. Chen, H.F. Cheng, and I.N. Lin, *J. Appl. Phys.*, **94**, 3360 (2003).
14. Y.C. Chen, H.F. Cheng, H.L. Liu, C.T. Chia, and I.N. Lin, *J. Appl. Phys.*, **94**, 3365 (2003).
15. A.C. Larson and R.B. Von Dreele, "General Structure Analysis System," Los Alamos National Laboratory Report LAUR, 86–748 (1994).
16. W.G. Spitzer, R.C. Miller, D.A. Kleinman, and L.E. Howarth, *Phys. Rev.*, **126**, 1710 (1962).